Double Torsion Coil Feeding Structure for Patch Antennas

Zhen-Yuan Zhang and Ke-Li Wu, *Fellow, IEEE*

***Abstract*— A new feeding structure for patch antennas is proposed in this paper. The feeding structure is formed by a double torsion coil (DTC) with one end electrically connected to the ground. The maximum stretch length of the coil is around half of the wavelength of the center frequency. The winding direction of the coil is reversed at the middle point of the coil. The DTC is able to produce two coaxial equivalent magnetic dipoles polarized in the same direction, which can not only excite the TM_{01} mode of a patch antenna but also create another resonance, leading to a wideband impedance bandwidth. The working mechanism is explained in this paper by physics intuition. To validate the new feeding structure, a linear-polarized and a dual-polarized patch antenna prototypes working in the 3.5 GHz band are designed, manufactured, and measured. It is found that the linear-polarized patch antenna can achieve a bandwidth of 25% standing-wave ratio (SWR < 2) and 9.5 dBi average gain with stable radiation patterns and low cross polarization over the impedance bandwidth. The new feeding structure has a high potential for wideband massive multiple-input and multiple-output (M-MIMO) arrays of 5G and future wireless communication systems.**

***Index Terms*— Broadband antenna, double torsion coil (DTC), feeding structure, low profile, magnetic dipole, patch antenna.**

I. Introduction

WITH the advantage of the simplicity for fabrication and moderate radiation performance for many low-profile applications, the patch antenna has been widely used in various niche applications, including conformal antennas on aircraft, large-scale scanning arrays, and low-profile antenna arrays for cellular wireless systems [1]. Needless to say, the patch antenna is one of the most commonly used antenna forms.

One of the design issues of patch antennas is its inherently narrow impedance bandwidth. Several useful methods to broaden the impedance bandwidth of a patch antenna have been developed [2]–[22]. It is found that increasing the height of the patch is a simple way to increase the impedance bandwidth of the patch antenna [2]. However, for a thick patch antenna fed by a probe, the inherent inductance brought by the feeding probe, thereby, limits the working bandwidth to less than 10% for the standing-wave ratio (SWR) < 2. Many other approaches are available to increase the working bandwidth. Introducing parasitic elements is an effective approach if the dimension permits [3]. By adding a parasitic element above a patch antenna resonator [4]–[7], the stacked structure can provide an impedance bandwidth of 15%, while the antenna size and the complexity of fabrication are also increased. With a U-shaped slot etched on the patch resonator [8]–[11], an impedance bandwidth of more than 30% can be achieved with the cost of increased cross polarization and distorted radiation patterns.

Actually, there is very rich literature for extending the impedance bandwidth of the patch antenna [12]–[22]. Because of the limited space, only some of the commonly used methods are reviewed here. Aperture-coupled patch antenna can achieve an impedance bandwidth of 10% [12]. When the resonating frequency of the aperture is close to that of the patch, the impedance bandwidth can be broadened to more than 20% [13]. The cavity-back version of the aperture-coupled patch antenna can overcome the shortcoming of back-lobe radiation of aperture-coupled patch antennas [14]. A simple and effective feeding approach is to use an "L"-shaped probe, reaching an impedance bandwidth of more than 30% [15]–[19]. However, a high cross polarization in the H-plane radiation patterns and the unstable mechanical structure of the L-probe spurred many innovative ideas to improve the feeding structure for the L-probe fed patch antenna. Among them, a wideband patch antenna fed by an S-shaped probe for suppressing cross polarization and broadening the bandwidth is proposed in [19]. The out-of-phase currents on the two arms of the S-shaped probe create two in-phase magnetic dipoles. The M-probe/strip fed patch antenna proposed in [20]–[22] is another scheme to restrain the cross polarization. Compared with the L-probe feeding method, the M-probe fed patch antenna is able to reduce the level of the cross polarization.

In this paper, a new broadband feeding configuration, namely, a double torsion coil (DTC) feeding structure, for patch antennas is proposed. The feeding structure can effectively create magnetic dipoles tangential to and immediately above the ground plane. The attractive features of the feeding structure include: 1) low profile; 2) mechanically stable; 3) wide impedance bandwidth; and 4) low cross polarization in both the E- and H-planes; and 5) generic for many other types of antennas. The magnetic dipole can not only excite the TM_{01} mode underneath the patch antenna but also create another resonant magnetic dipole in a neighboring frequency, leading to a wideband impedance bandwidth.

To validate the proposed feeding structure, a singly fed linearly polarized patch antenna and a dual linearly polarized patch antenna are electromagnetic (EM) designed and

Manuscript received October 11, 2018; revised February 19, 2019; accepted February 27, 2019. Date of publication March 18, 2019; date of current version May 31, 2019. This work was supported by The Chinese University of Hong Kongthrough the Postgraduate Scholarship. *(Corresponding author: Ke-Li Wu.)*

The authors are with the Department of Electronic Engineering, The Chinese University of Hong Kong, Sha Tin, Hong Kong (e-mail: zyzhang@ee.cuhk.edu.hk; klwu@ee.cuhk.edu.hk).

Color versions of one or more of the figures in this paper are available online at http://ieeexplore.ieee.org.

Digital Object Identifier 10.1109/TAP.2019.2905791

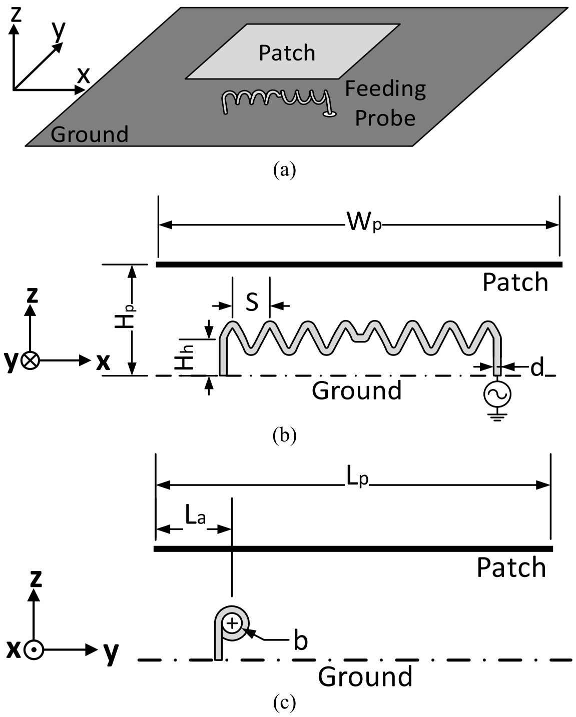

Fig. 1. (a) Isometric view of an air patch antenna fed by the proposed DTC. (b) Front view. (c) Side view.

prototyped. The electrical dimensions of the linearly polarized prototype antenna are about $0.39\lambda_o \times 0.39\lambda_o \times 0.08\lambda_o$, where λ_o is the free-space wavelength at the center frequency. The impedance bandwidth of more than 25% for SWR less than 2 and the measured average gain of 9.5 dBi over the working frequency band can be achieved. The radiation patterns are stable, and the cross polarization is very low both in the E- and H-planes over the matched impedance frequency band. The dual linearly polarized prototype antenna demonstrates that the DTC feeding structure can find many practical applications, including compact dual-polarized array antennas for massive multi-in multi-out (M-MIMO) base stations.

II. Configuration and Working Mechanism

A. Feeding Configuration for Patch Antennas

The detailed configuration of the proposed feeding structure for a singly fed linearly polarized patch antenna is illustrated in Fig. 1. The feeding structure is a DTC with one end shorted to the ground and the other end is excited by a coaxial cable. The maximum stretch length of the conducting coil is around half a wavelength at the center frequency. It is called a DTC because the winding directions of the first half and the second half are the opposite from each other. Having wound in two opposite directions, the two half-coils produce two equivalent magnetic dipoles tangential to and above the ground plane in the same direction.

The length and width of the patch antenna are L_p and W_p, respectively. The patch is placed at height H_p above the ground plane. The proposed DTC feeding structure is grounded at one end and excited at the other end. The coil is made of a piece of conductor wire of diameter d. The distance between the axis of the coil and the ground plane is H_h. The

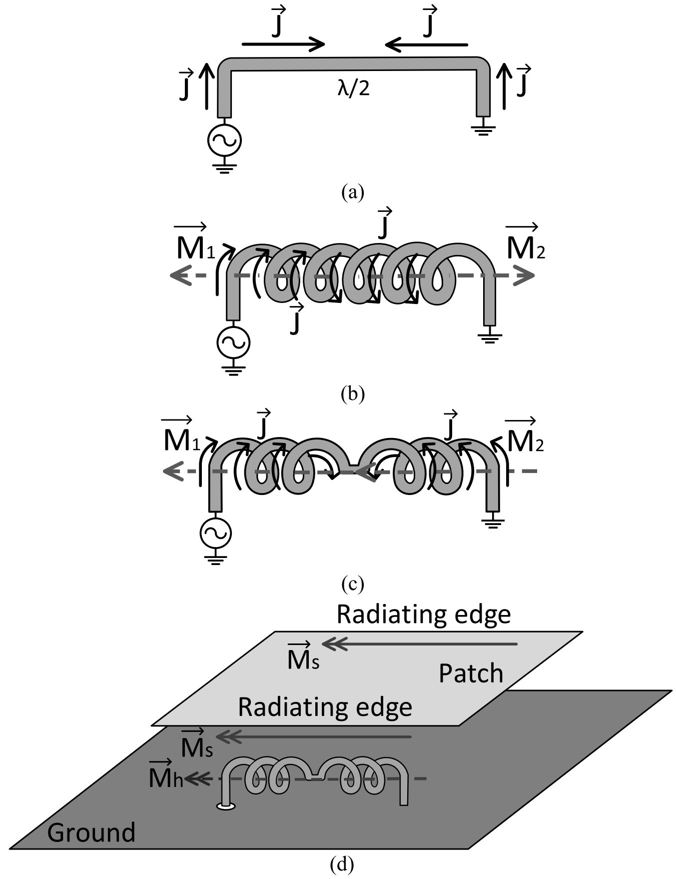

Fig. 2. Working mechanism of the DTC feeding structure to the patch antenna. (a) Distribution of electric current on a straight metal wire with one end grounded. (b) Distribution of electric current on a single torsion coil with one end grounded and its equivalent magnetic dipole. (c) Distribution of electric current and magnetic dipole on a DTC with one end grounded. (d) Coupling of a DTC feeding probe and a radiating patch.

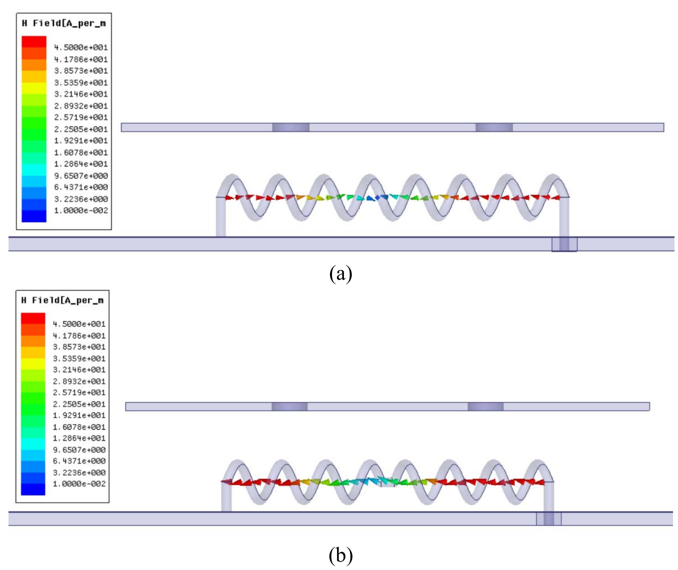

Fig. 3. Distribution of magnetic field along the axis of (a) single torsion coil and (b) DTC.

coil is with an inner radius of b and pitch of S. The coil is located at the middle of the patch antenna and L_a distance inward from one radiating edge of the patch antenna. Usually,

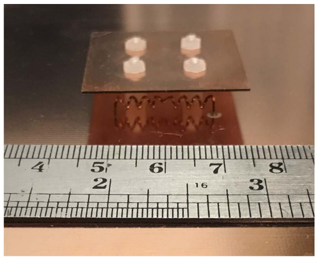

Fig. 4. Photograph of a linearly polarized air patch antenna with DTC feeding structure.

TABLE I
DIMENSIONS OF THE LINEARLY POLARIZED PROTOTYPE ANTENNA

	L_p	W_p	H_p	L_a	H_h	b	d	S
mm	32	32	6.2	3	2.3	0.8	0.6	2.7
λ_o	0.39	0.39	0.07	0.04	0.03	0.01	0.01	0.03

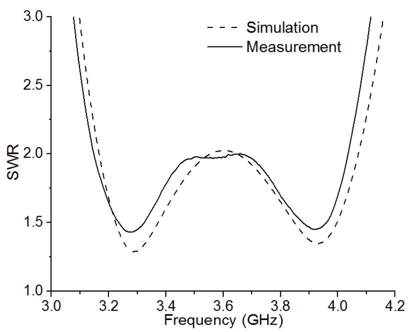

Fig. 5. Simulated and measured SWR of the linearly polarized patch antenna.

TABLE II
MEASURED X-POL, 3 dB BEAMWIDTH, AND F/B RATIO OF THE LINEARLY POLARIZED PROTOTYPE ANTENNA

Frequency (GHz)	X-pol Level (dB)		3-dB Beam-width		F/B Ratio (dB)
	0°	±60°	E-plane	H-plane	
3.2	-25	-15	68°	72°	19
3.6	-27	-16	56°	73°	22
4.0	-27	-13	48°	75°	20

the distance L_a is very small. The number of turns N of the half coil is selected as 3.5. By designing the geometric parameters appropriately, the coil can effectively excite the radiating patch.

B. Working Mechanisms

In this section, the working mechanism of the DTC feeding structure will be explained. Fig. 2(a) illustrates the direction of electric current on a straight conducting wire with one end grounded if the total length of the wire is approximately $\lambda_o/2$, where λ_o is the free-space wavelength at the resonant frequency. It can be seen that there is a current null in the middle point of the wire, at which the direction of the current is reversed. If the straight wire is wound in one direction to form an ordinary single torsion coil, the direction of the current along the wire will be also reversed, as shown in Fig. 2(b), leading to two same magnitude but opposite directed equivalent magnetic dipoles. Thus, the contributions

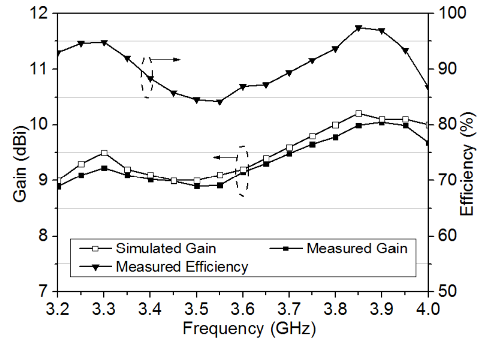

Fig. 6. Simulated and measured gain and efficiency of the linearly polarized patch antenna.

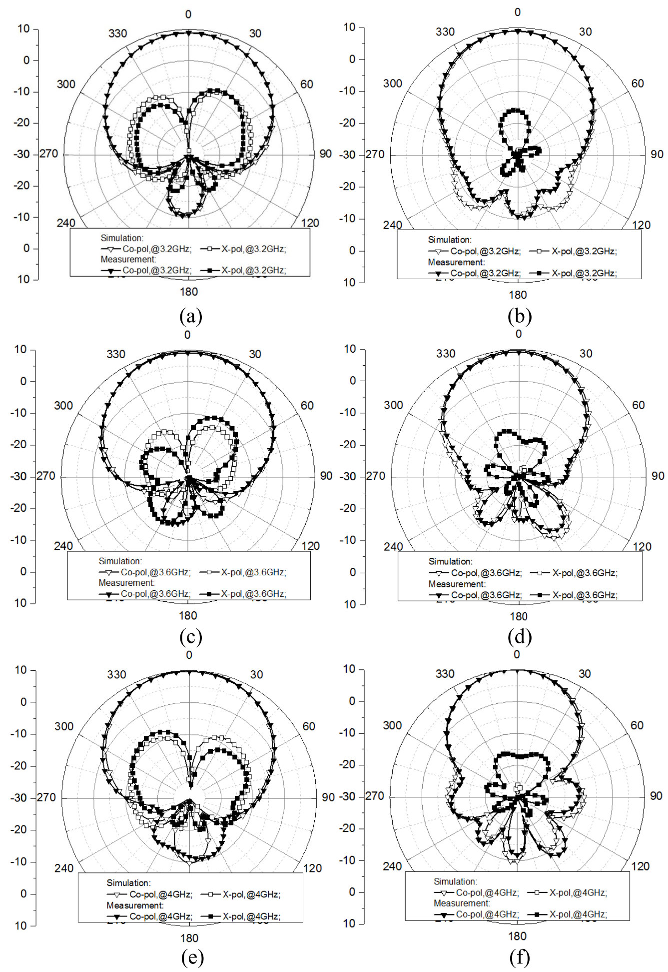

Fig. 7. Simulated and measured radiation patterns of the linearly polarized patch antenna at 3.2, 3.6, and 4.0 GHz for (a), (c), (e) H-plane and (b), (d), (f) E-plane.

of the two magnetic dipoles to the far field cancel each other. The direction of the equivalent magnetic dipole created by a coil depends on two factors: the direction of the current along the helical wire and the winding direction of the coil. Although the current direction on the coil is reversed, to create two magnetic dipoles with the same direction, the winding directions of the first half and the second half of the coil need to be opposite, as shown in Fig. 2(c). It is known that the patch antenna can be described by two radiating magnetic dipoles in line with the two radiating edges. As illustrated

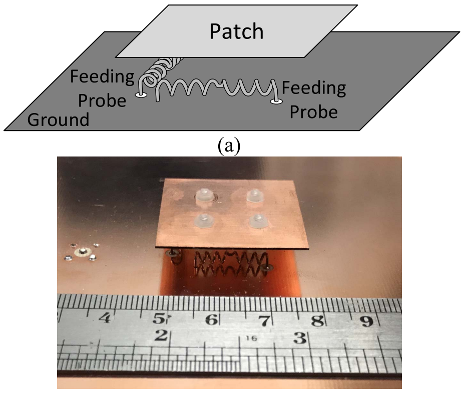

Fig. 8. (a) Isometric view and (b) photograph of the dual-polarized patch antenna with the DTC feeding structure.

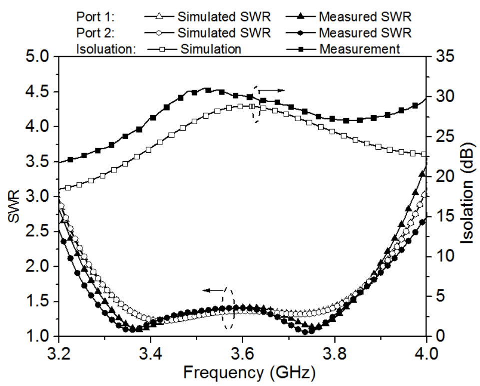

Fig. 9. Simulated and measured SWR and isolation of the proposed dual-polarized prototype antenna.

TABLE III

DIMENSIONS OF THE DUAL-POLARIZED PROTOTYPE ANTENNA

	L_p	W_p	H_p	L_a	H_h	b	d	S
mm	32	32	5.8	2.75	1.75	0.8	0.6	2.1
λ_o	0.39	0.39	0.07	0.03	0.02	0.01	0.01	0.03

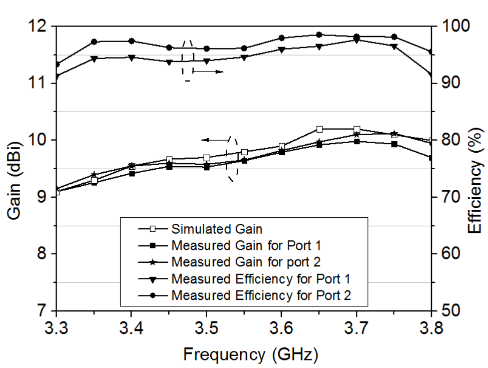

Fig. 10. Simulated and measured gain and efficiency of the dual-polarized prototype antenna.

in Fig. 2(d), the aggregated magnetic dipole created by the DTC can be naturally coupled with a radiating magnetic dipole of the patch. For a horizontally placed magnetic dipole

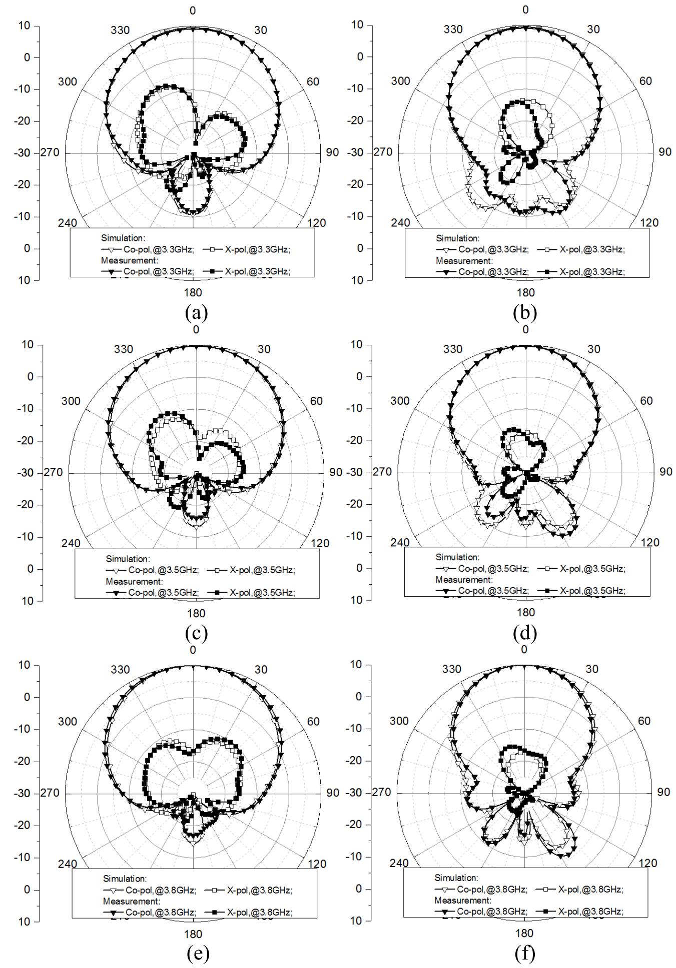

Fig. 11. Simulated and measured radiation patterns of the dual-polarized prototype antenna at 3.3, 3.5, and 3.8 GHz for (a), (c), (e) H-plane and (b), (d), (f) E-plane.

TABLE IV

MEASURED X-POL, 3 dB BEAMWIDTH, AND F/B RATIO OF THE DUAL-POLARIZED PROTOTYPE ANTENNA

Frequency (GHz)	X-pol level (dB)		3-dB beam width		F/B Ratio (dB)
	0°	±60°	E-plane	H-plane	
3.2	-25	-15	58°	74°	20
3.5	-28	-15	52°	72°	18
4.0	-27	-16	50°	76°	18

above the ground plane, its mirror image will be in the same direction, constructively contributing to the far field. This feature permits the coil to be placed very close to the ground. The simulated magnetic fields along the axis of a single torsion coil and DTC are shown in Fig. 3(a) and (b), justifying the concept that the magnetic dipoles produced by the DTC share the same direction. By choosing the maximum stretch length of the coil approximately to be $\lambda_o/2$, the DTC feeding structure acts as a magnetic dipole antenna in free space, creating additional resonance to the patch antenna.

III. ANTENNA EXAMPLES

To validate the proposed feeding structure and demonstrate its applicability in a practical dual-polarized patch

TABLE V

COMPARISON OF DTC FED AIR PATCH ANTENNA WITH EXISTING BROADBAND PATCH ANTENNAS

Ref (Year)	Configuration	Antenna Dimensions		Bandwidth		Average Gain (dBi)	X-Pol level (dB) 0^o / $\pm 60^o$	F/B Ratio (dB)
		Physical (mm^3)	Electrical (λ_o)	Impedance Bandwidth (GHz) (%)	1-dB Gain Bandwidth (%)			
[9] (2000)	U-slot patch antenna	36 × 26 × 8	0.38 × 0.27 × 0.09	2.7-3.56 (SWR < 2) (27%)	> 26.7%	6.5	N/A	> 12.7
[17] (2001)	L-probe fed patch antenna	30 × 25 × 6.6	0.45 × 0.375 × 0.1	3.8–5.4 (SWR < 2) (36%)	36%	6	< - 10 / < 0	> 19
[19] (2018)	Antisymmetric L-probe fed patch antenna	50 × 50 × 24	0.38 × 0.38 × 0.17	1.71–2.83 (SWR < 2) (49.3%)	~27%	9	< - 30 / < -5	> 19.5
[20] (2006)	M-probe fed patch antenna	60 × 70 × 17.5	0.36 × 0.43 × 0.1	1.6–2.05(SWR < 1.5) (24%)	> 24%	9	< - 18 / < - 10	> 19
[14] (1990)	Aperture-coupled patch antenna	17 × 17 × 7.1	0.32 × 0.32 × 0.13	4.85-6.1 (SWR < 1.5) (22%)	N/A	8	< - 40 / < - 15	> 14
This Work	Double torsion coil fed patch antenna	32 × 32 × 6.2	0.38 × 0.38 × 0.07	3.15 - 4.05 (SWR < 2) (25%)	> 25%	9.5	< - 25 / < - 13	> 19

antenna for an M-MIMO array antenna, linearly polarized and dual-polarized prototype antennas are designed, fabricated, and fully tested. The working frequency band of the linearly polarized antenna spans from 3.15 to 4.05 GHz, achieving a wide impedance bandwidth of 25% (for SWR $<$ 2). The dual-polarized prototype antenna achieves an impedance bandwidth of 16.3% (for SWR $<$ 1.5). For both prototypes, the size of the ground plane is chosen to be 120 × 120 mm^2. All the radiation properties are measured using the SATIMO SG-128 spherical scanner system in the Radio-frequency Radiation Research Laboratory (R3L) of the university.

A. Prototype of Linearly Polarized Patch Antenna

A prototype of a linearly polarized patch antenna with the proposed DTC feeding structure, as shown in Fig. 4, is designed and measured. The overall electrical size of the patch antenna is $0.39\lambda_o \times 0.39\lambda_o \times 0.079\lambda_o$ and its physical dimensions are listed in Table I. The HFSS EM simulated and measured SWR of the prototype antenna are superimposed in Fig. 5, showing good agreement. The bandwidth for SWR $<$ 2 is about 25%, which spans from 3.15 to 4.05 GHz.

The simulated and measured antenna gains and the measured radiation efficiency are superimposed in Fig. 6, showing that the measured average gain of the antenna is about 9.5 dBi and the measured maximum gain is about 10 dBi. The measured average radiation efficiency of the linearly polarized patch antenna is better than 85%. The simulated and measured radiation patterns at 3.2, 3.6, and 4 GHz are plotted in Fig. 7, showing very good agreement between the simulated and the measured. The measured cross polarization (X-pol) level, 3 dB beamwidth, and front/back (F/B) radiation ratio measured at 3.2, 3.6, and 4 GHz are listed in Table II, showing that the cross-polarization level is low and the F/B ratio is maintained at a high level over the working bandwidth.

B. Prototype of Dual Linearly Polarized Patch Antenna

A dual linearly polarized patch antenna with two DTC feeding structures is sketched in Fig. 8(a). Fig. 8(b) is a photograph of the finished prototype. The physical dimensions of the finished antenna prototype are listed in Table III. The overall size of the antenna prototype is about $0.39\lambda_o \times 0.39\lambda_o \times 0.07\lambda_o$. The simulated and measured S-parameters of the prototype antenna are superposed in Fig. 9. The bandwidth for SWR $<$ 1.5 spans from 3.27 to 3.85 GHz or 16.3% fractional bandwidth, within which the measured port isolation is better than 25 dB.

The simulated and measured antenna gains and the measured radiation efficiencies of both ports are shown in Fig. 10. In measuring one port, the other port is terminated by a matched load. The measured antenna gain varies from 9 to 10 dBi within the impedance bandwidth. The measured radiation efficiency is better than 90%. Because of the symmetry of the antenna structure, only the simulated and measured radiation patterns of port 1 at 3.3, 3.5, and 3.8 GHz are presented in Fig. 11. The measured cross polarization (X-pol), 3 dB beamwidth, and F/B ratio at 3.3, 3.5, and 3.8 GHz are listed in Table IV.

A comparison of various patch antennas using the proposed DTC feeding structure and other means of expanding the bandwidth is presented in Table V. It can be observed that the DTC feeding structure does not affect the patch dimensions L_p and W_p, which are comparable to those wideband air patch, but the height of the patch antenna is less. Because of the creation of the magnetic dipole, the DTC fed patch antenna achieves the lowest profile among all the designs. For the L-probe feeding structure, a large X-pol level in the H-plane may be attributed by the vertical component of the current on the probe [16]. The proposed magnetic dipole exhibits less vertical electric current component. Therefore, the cross polarization of the patch antenna is weaker than that of most of the wideband designs [9], [17], [20]. As a side notes, the radiation gain and 3 dB beamwidth are also comparable to those of the other wideband antenna configurations.

IV. PARAMETRIC STUDY

In this section, the variation of the antenna characteristics with dimensional parameters, including the pitch of the coil S, the length of the patch L_p, the height of the patch H_p,

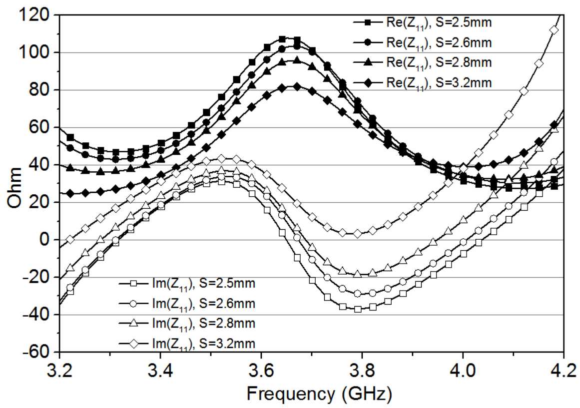

Fig. 12. Input impedance versus pitch S with other dimensions listed in Table II.

TABLE VI
DIMENSIONS OF THE ANTENNAS FOR CURVES IN FIG. 12(B) AND (C)

	H_p (mm)	*b (mm)*	*S (mm)*	*N*
Fig. 13(b)	6.2	0.6	3.9	3.5
	6.2	0.7	3.3	3.5
	6.2	0.8	2.7	3.5
	7	0.9	2	3.5
	7	1	1.4	3.5
Fig. 13(c)	6.5	1.2	2.5	2.5
	6.2	0.8	2.7	3.5
	6.8	0.8	1.5	4.5

the inner radius of the coil b, and the number of the turns of the coil N, is investigated using HFSS EM simulation. The variation of the radiation characteristics of the antenna, including X-pol level and F/B ratio with the height of the coil H_h is also discussed.

The variation of the input impedance, $Re(Z_{11})$ and $\mathrm{Im}(Z_{11})$, with the pitch S is illustrated in Fig. 12. Other dimensions are the same as those provided in Table I. It can be observed that when S is increased, the input impedance turns to be more inductive. The variation of SWR by changing the height of the patch antenna H_p is shown in Fig. 13(a): the working bandwidth is controlled by the height of the patch. Other dimensions are the same as those provided in Table I. The bandwidth defined by SWR < 2 changes from 0.9 to 0.56 GHz when the height H_p changes from 6.2 to 8.2 mm. It is intuitive that the spacing between the coil and the patch mainly controls the mutual coupling between the coil and the patch resonator. The smaller the spacing, the stronger the coupling is. Fig. 13(b) shows the variation of the SWR with different values of the inner radius b. The corresponding dimensions are listed in Table VI, while other dimensions are the same as those provided in Table I. It can be seen that when b equals to 0.8 mm, the optimal working bandwidth can be achieved. As shown in Table VI, when the inner radius of the coil is small, to maintain the resonant length of approximately $\lambda_o/2$, the pitch S needs to be large. When the radius of the coil is large, it is noticed that the height of the patch should be large too, which means the increase in b will enlarge the coupling between the coil and the patch. The variation of the SWR with the number of turns N is shown in Fig. 13(c): when N is small, the radius of the coil b and the pitch S become large to maintain the maximum stretch length of about a half of λ_o. According to the height and the impedance bandwidth of the patch antenna, the optimal N is selected to be 3.5.

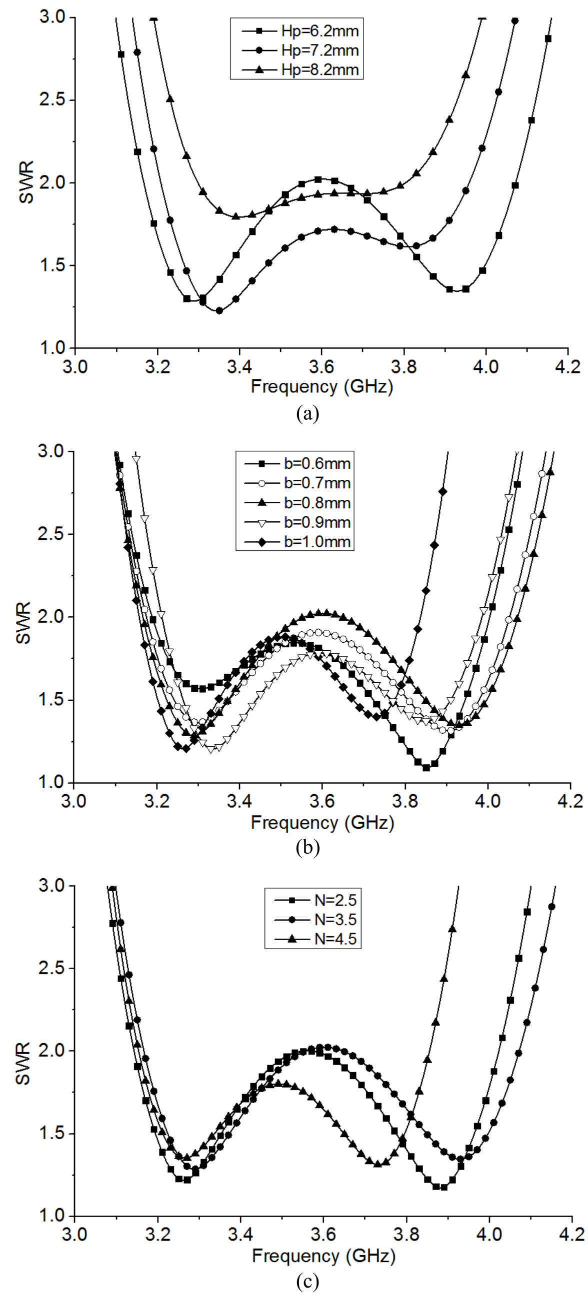

Fig. 13. SWR versus physical parameters of the linearly polarized patch antenna. (a) Height H_p. (b) Inner radius b of the coil. (c) Number of turns N of the coil.

The H-plane radiation patterns simulated at 3.5 GHz with different heights of the coil are superimposed in Fig. 14, showing that when the height of the coil increases, the X-pol level turns to be worse a little bit, especially in the large elevating angle. However, increasing the height improves the F/B ratio.

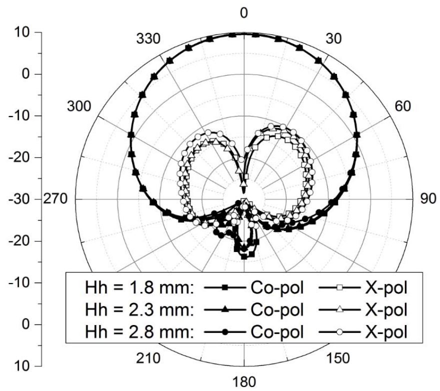

Fig. 14. H-plane radiation pattern of the linearly polarized patch antenna versus the height of the coil H_h with other dimensions listed in Table I.

V. Conclusion

In this paper, a new feeding structure for the patch antenna is proposed by creating an equivalent magnetic dipole that is tangential to and slightly above the ground plane. The feeding structure is formed by the DTC with one end grounded and the other end excited by a coaxial cable. The maximum stretch length of the coil is about half a wavelength at the center frequency. The tuning directions of the first half and the second half are opposite. The magnetic dipole created by the DTC can not only excite the TM_{01} mode of the patch antenna but also create another resonance, leading to a wideband impedance bandwidth. Since a magnetic dipole can be placed tangentially to the ground plane closely, the proposed feeding structure to a patch antenna can be low profile. For an air patch antenna of height $0.07\lambda_o$, a typical impedance bandwidth of 24% for SWR < 2 can be achieved with an average gain of 9.5 dBi. The feeding structure can be easily used to feed a dual linearly polarized patch antenna and other types of antenna elements, providing a new feeding mechanism for wideband M-MIMO array antennas in 5G and future wireless communication systems.

References

[1] J. R. James and P. S. Hall, *Handbook of Microstrip Antennas*. London, U.K.: Peter Peregrinus Ltd., 1989.

[2] D. H. Schaubert, D. M. Pozar, and A. Adrian, "Effect of microstrip antenna substrate thickness and permittivity: Comparison of theories with experiment," *IEEE Trans. Antennas Propag.*, vol. 37, no. 6, pp. 677–682, Jun. 1989.

[3] C. Wood, "Improved bandwidth of microstrip antennas using parasitic elements," *Proc. Inst. Elect. Eng.–H, Microw. Opt. Antennas*, vol. 127, no. 4, pp. 231–234, Aug. 1980.

[4] L. Barlately, J. R. Mosig, and T. Sphicopoulos, "Analysis of stacked microstrip patches with a mixed potential integral equation," *IEEE Trans. Antennas Propag.*, vol. 38, no. 5, pp. 608–615, May 1990.

[5] R. Q. Lee, K. F. Lee, and J. Bobinchak, "Characteristics of a two-layer electromagnetically coupled rectangular patch antenna," *Electron. Lett.*, vol. 23, no. 20, pp. 1070–1073, Sep. 1987.

[6] A. N. Tulintseff, S. M. Ali, and J. A. Kong, "Input impedance of a probe-fed stacked circular microstrip antenna," *IEEE Trans. Antennas Propag.*, vol. 39, no. 3, pp. 382–390, Mar. 1991.

[7] K. F. Lee, W. Chen, and R. Q. Lee, "Studies of stacked electromagnetically coupled patch antennas," *Microw. Opt. Tech. Lett.*, vol. 8, no. 4, pp. 212–215, Mar. 1995.

[8] T. Huynh and K.-F. Lee, "Single-layer single-patch wideband microstrip antenna," *Electron. Lett.*, vol. 31, no. 16, pp. 1310–1312, Aug. 1995.

[9] K.-F. Tong, K.-M. Luk, K.-F. Lee, and R. Q. Lee, "A broad-band U-slot rectangular patch antenna on a microwave substrate," *IEEE Trans. Antennas Propag.*, vol. 48, no. 6, pp. 954–960, Jun. 2000.

[10] R. Chair, C.-L. Mak, K.-F. Lee, K.-M. Luk, and A. A. Kishk, "Miniature wide-band half U-slot and half E-shaped patch antennas," *IEEE Trans. Antennas Propag.*, vol. 53, no. 8, pp. 2645–2652, Aug. 2005.

[11] K. F. Lee, S. L. Yang, A. A. Kishk, and K. M. Luk, "The versatile U-slot patch antenna," *IEEE Antennas Propag. Mag.*, vol. 52, no. 1, pp. 71–78, Feb. 2010.

[12] D. M. Pozar, "Microstrip antenna aperture-coupled to a microstripline," *Electron. Lett.*, vol. 21, no. 1, pp. 49–50, Jan. 1985.

[13] F. Croq and A. Papiernik, "Large bandwidth aperture-coupled microstrip antenna," *Electron. Lett.*, vol. 26, no. 16, pp. 1293–1294, Aug. 1990.

[14] S. D. Targonski, R. B. Waterhouse, and D. M. Pozar, "Design of wide-band aperture-stacked patch microstrip antennas," *IEEE Trans. Antennas Propag.*, vol. 46, no. 9, pp. 1245–1251, Sep. 1998.

[15] K. M. Luk, C. L. Mak, Y. L. Chow, and K. F. Lee, "Broadband microstrip patch antenna," *Electron. Lett.*, vol. 34, no. 15, pp. 1442–1443, Jul. 1998.

[16] C. L. Mak, K. M. Luk, K. F. Lee, and Y. L. Chow, "Experimental study of a microstrip patch antenna with an L-shaped probe," *IEEE Trans. Antennas Propag.*, vol. 48, no. 5, pp. 777–783, May 2000.

[17] Y.-X. Guo, C.-L. Mak, K.-M. Luk, and K.-F. Lee, "Analysis and design of L-probe proximity fed-patch antennas," *IEEE Trans. Antennas Propag.*, vol. 49, no. 2, pp. 145–149, Feb. 2001.

[18] C.-L. Mak, H. Wong, and K.-M. Luk, "High-gain and wide-band single-layer patch antenna for wireless communications," *IEEE Trans. Veh. Technol.*, vol. 54, no. 1, pp. 33–40, Jan. 2005.

[19] K. M. Mak, H. W. Lai, and K. M. Luk, "A 5G wideband patch antenna with antisymmetric L-shaped probe feeds," *IEEE Trans. Antennas Propag.*, vol. 66, no. 2, pp. 957–961, Feb. 2018.

[20] H.-W. Lai and K.-M. Luk, "Design and study of wide-band patch antenna fed by meandering probe," *IEEE Trans. Antennas Propag.*, vol. 54, no. 2, pp. 564–571, Feb. 2006.

[21] H.-W. Lai and K.-M. Luk, "Wideband patch antenna FED by printed meandering strip," *Microw. Opt. Tech. Lett.*, vol. 50, no. 1, pp. 188–192, Jan. 2008.

[22] H.-W. Lai and K.-M. Luk, "Dual polarized patch antenna fed by meandering probes," *IEEE Trans. Antennas Propag.*, vol. 55, no. 9, pp. 2625–2627, Sep. 2007.

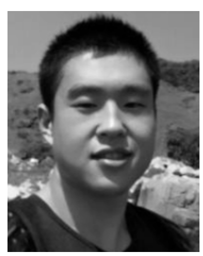

Zhen-Yuan Zhang was born in Changzhou, Jiangsu, China, in 1988. He received the B.S. degree in electronic science and engineering from the Nanjing University of Posts and Communications, Nanjing, China, in 2011, and the M.S. degree in electronic engineering from The Chinese University of Hong Kong, Hong Kong, in 2013, where he is currently pursuing the Ph.D. degree in electronic engineering.

His current research interests include circularly polarized antenna design, wideband base station antenna design, and antenna decoupling techniques.

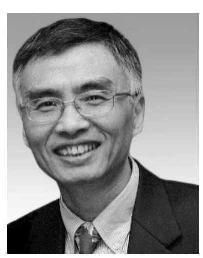

Ke-Li Wu (M'90–SM'96–F'11) received the B.S. and M.Eng. degrees from the Nanjing University of Science and Technology, Nanjing, China, in 1982 and 1985, respectively, and the Ph.D. degree from Laval University, Quebec City, QC, Canada, in 1989.

From 1989 to 1993, he was a Research Engineer with McMaster University, Hamilton, ON, Canada. In 1993, he joined COM DEV (now Honeywell Aerospace), Cambridge, ON, Canada, where he was a Principal Member of Technical Staff. Since 1999, he has been with The Chinese University of Hong Kong, Hong Kong, where he is currently a Professor and the Director of the Radio-frequency Radiation Research Laboratory. His current research interests include electromagnetic (EM)-based circuit domain modeling of high-speed interconnections, robot automatic tuning of microwave filters, decoupling techniques of MIMO antennas, and Internet of Things technologies.

Dr. Wu is a member of the IEEE MTT-8 Subcommittee. He serves as a TPC member for many prestigious international conferences. He was a recipient of the 1998 COM DEV Achievement Award and the Asia–Pacific Microwave Conference Prize twice in 2008 and 2012, respectively. He was an Associate Editor of the IEEE Transactions on Microwave Theory and Techniques from 2006 to 2009.